

Homotopic topological phases of matter in two dimensions: theory and application to Sr_2RuO_4

A. M. Cook¹

¹*Department of Physics, University of California, Berkeley, California, 94720, USA*

We introduce two-dimensional topological phases of matter defined by non-trivial homotopy groups into the literature, characterized either by a single Skyrmion number, known as the chiral topological Skyrmion insulator, or a pair of Skyrmion numbers, known as the helical topological Skyrmion insulator, which generalize and extend the concepts of the Chern insulator and quantum spin Hall insulator, respectively. We show each topological phase of matter is protected by a combination of a mirror symmetry and a generalized particle-hole symmetry equal to the product of particle-hole symmetry and spatial inversion symmetry. Despite these phases being protected in part by crystalline point group symmetries, the phases introduced here are very different from all others known: we characterize three kinds of phase transitions by which a Skyrmion number can change, with one being a topological phase transition that occurs without the closing of energy gaps, which has important consequences for study of topologically non-trivial phases of matter. We find that each phase is realized in a tight-binding model relevant to Sr_2RuO_4 and discuss possible experimental realization given that the chiral topological Skyrmion insulator phase is realized for a parameter set used to characterize Sr_2RuO_4 .

The search for topologically non-trivial phases of matter is now a vast and influential topic in condensed matter physics. One of the most important concepts in this research domain is that of the Chern insulator [1], a two-dimensional topologically non-trivial phase of matter central to the construction of many others, from the quantum spin Hall insulator [2–6] and the Weyl semimetal [7–13], to topological crystalline phases of matter [14–19], to topological phases in non-electronic systems [20–23] and systems out of equilibrium, such as the Floquet topological phases [24–33], and dissipative systems, such as the non-Hermitian topological phases [34–40].

In this work, we identify and characterize a foundational generalization and counterpart of the Chern insulator, starting from the following concept: the simplest models for Chern insulators are one-electron Hamiltonians with $2N \times 2N$ matrix representations and $N = 1$. The topology of the Chern insulator is characterized by the first Chern number, computed for the single occupied band when $N = 1$. This topological invariant is also, in this situation, the Skyrmion number, the topological charge of the momentum space ground state spin texture (or pseudospin texture depending on the degree of freedom in the model).

For $N > 1$, however, this equivalence between the Chern number and the Skyrmion number breaks down. For $N > 1$, Chern insulators are characterized by a total Chern number C of the occupied bands, computed as the sum of the first Chern numbers of individual occupied bands. The Skyrmion number Q , in contrast, is a global topological invariant [41] and an example of a topological invariant classifying topologically-distinct maps from the Brillouin zone torus T^k to a space M , corresponding to non-trivial homotopy group $\pi_k(M) \neq 0$. Thus, while the Chern number and the Skyrmion number are locked together for $N = 1$, the Skyrmion number characterizes topological phases of matter distinct from the Chern insulator for $N > 1$ that we introduce in this work. As the topology of these phases of matter is characterized by homotopy invariants, so we denote these two-dimensional phases of matter by *homotopic topological insulators*.

We present results on two symmetry-protected topological phases of matter. First, we introduce two-dimensional *chiral homotopic topological insulators* characterized by the

Skyrmion number, or *chiral topological Skyrmion insulators* (CTSIs). These topological phases of matter are characterized by a single Skyrmion number. Second, we present results on two-dimensional *helical homotopic topological insulators* characterized by a pair of Skyrmion numbers, or *helical topological Skyrmion insulators* (HTSIs). In these cases where $N > 1$ and specifically for Hamiltonians with $2N \times 2N$ matrix representations corresponding to homotopy group $\pi_2(\text{Sp}(2N)/U(N)) = \mathbb{Z}$, we find the Skyrmion number in two dimensions can be an integer-quantized global invariant distinct from the total Chern number computed as the sum of the Chern numbers of individual bands over the set of occupied bands. Phases of matter characterized by non-trivial Skyrmion numbers can therefore be distinct from Chern insulators contrary to intuition based on the $N = 1$ case.

Achieving $\pi_k(M) \neq 0$ for $N > 1$ is a largely unexplored topic. Past work has considered the role of \mathcal{C}' symmetry in realizing Hamiltonians corresponding to $\pi_3(\text{Sp}(2N)/U(N))$ and $\pi_4(\text{Sp}(2N)/U(N))$, realizing counterparts of the Hopf insulator [42] in abstract models. Here, we find evidence that both the chiral and helical topological Skyrmion insulator phases are realized in a model previously used to describe the superconductor Sr_2RuO_4 in the high-field phase, and that Sr_2RuO_4 specifically is a candidate for the chiral topological Skyrmion insulator phase. This work introduces methods for constructing and characterizing these phases and serves as a starting point in searching for homotopic topological phases of matter in other superconductors and strongly-correlated materials.

Topological classification of chiral topological Skyrmion insulators.—We first review and extend work by Xu and co-authors [42] to show a generalized particle-hole symmetry \mathcal{C}' is desired for realization of the homotopy group $\pi_2(\text{Sp}(2N)/U(N))$. From work by Bott [43], we have the following relation between homotopy groups, where Sp is the symplectic group and U is the unitary group,

$$\pi_k(\text{Sp}/\text{U}) = \pi_{k+1}(\text{Sp}). \quad (1)$$

Xu and co-authors [42] use this relation in combination with work on the homotopy groups of symplectic

groups [44] to determine the topological classification of the set of Hamiltonians they present, with homotopy group $\pi_3(Sp(2N)/U(N))$, to be \mathbb{Z}_2 for $N > 1$. They also briefly consider $\pi_4(Sp(2N)/U(N))$.

To understand whether the generalized particle-hole symmetry \mathcal{C}' is desired in the case of a two-dimensional Brillouin zone for Hamiltonians to be topologically-classified by homotopy group $\pi_2(Sp(2N)/U(N))$, we consider a Hamiltonian $H(\mathbf{k})$ possessing \mathcal{C}' symmetry. $H(\mathbf{k})$ therefore satisfies

$$\mathcal{J}^{-1}H(\mathbf{k})\mathcal{J} = -H^*(\mathbf{k}) \quad (2)$$

for each \mathbf{k} , with $\mathcal{J} = \begin{pmatrix} 0 & I_{N \times N} \\ -I_{N \times N} & 0 \end{pmatrix}$, where $I_{N \times N}$ is the $N \times N$ identity matrix. This constraint on the Hamiltonian for each \mathbf{k} restricts the set of Hamiltonians permitted to the symplectic group, Sp, and also forces the number of bands of the Hamiltonian to be even.

A generic element that does not move $I_{N \times N}$ is $g = \text{diag}(U_1(\mathbf{k}), U_2(\mathbf{k}))$, where $U_1(\mathbf{k}), U_2(\mathbf{k}) \in U(N)$. For g to be in $Sp(2N)$, it must satisfy

$$\begin{pmatrix} U_1 & 0 \\ 0 & U_2 \end{pmatrix} \mathcal{J} \begin{pmatrix} U_1 & 0 \\ 0 & U_2 \end{pmatrix}^T = \mathcal{J}. \quad (3)$$

For this expression to hold, $U_1 U_2^T = I$, where I is the identity matrix. This corresponds to the configuration space of the Hamiltonian being $Sp(2N)/U(N)$. Xu's discussion [42] holds whether we consider a three-dimensional Brillouin zone or a two-dimensional one. Thus, we expect Hamiltonians with two-dimensional Brillouin zones and \mathcal{C}' symmetry to have \mathbb{Z} topological classification characterized by a global homotopy invariant.

Topological invariant of the \mathcal{C}' insulator in two dimensions.—The constraints on g due to \mathcal{C}' symmetry mean U_1 and U_2 are furthermore restricted to $SU(N)$, guaranteeing the existence of a three-vector with which the homotopy invariant may be computed. For a three-dimensional Brillouin zone in certain simplified cases, this homotopy invariant is the topological charge of a three-dimensional skyrmion [42, 45]. For a two-dimensional Brillouin zone as we consider, the homotopy invariant is the Skyrmion number \mathcal{Q} of the momentum-space ground state spin or pseudospin texture [46], expressed as an integral over the two-dimensional Brillouin zone,

$$\mathcal{Q} = \frac{1}{4\pi} \int_{BZ} \Omega_{\hat{\mathcal{S}}}(\mathbf{k}) d^2k, \quad (4)$$

where $\Omega_{\hat{\mathcal{S}}}(\mathbf{k}) = \hat{\mathcal{S}}(\mathbf{k}) \cdot (\partial_{k_x} \hat{\mathcal{S}}(\mathbf{k}) \times \partial_{k_y} \hat{\mathcal{S}}(\mathbf{k}))$ is expressed in terms of the normalized ground state spin expectation value $\hat{\mathcal{S}}(\mathbf{k}) = \mathcal{S}(\mathbf{k})/|\mathcal{S}(\mathbf{k})|$.

In this work, we consider topological phases of matter characterized by a single non-trivial Skyrmion number, $\mathcal{Q} \neq 0$, which we call a *chiral homotopic topological insulator* phase of matter, as well as a topological phase of matter consisting of a pair of decoupled homotopic topological insulators, one

with Skyrmion number $\mathcal{Q} \neq 0$ and the other with Skyrmion number $-\mathcal{Q}$, which we call a *helical homotopic topological insulator* phase of matter. We find both topologically non-trivial phases of matter are realized in a tight-binding model for Sr_2RuO_4 , with the chiral homotopic topological phase realized for a parameter set previously used to describe Sr_2RuO_4 specifically.

Construction of the helical homotopic topological phase utilizing mirror symmetry.—First, we consider a schematic model for a two-dimensional superconductor in the $x - y$ -plane with Bogoliubov-de Gennes (BdG) Hamiltonian as in Ueno *et al.* [47], expressed as

$$\mathcal{H} = \sum_{\mathbf{k}} \Psi_{\mathbf{k}}^\dagger \mathcal{H}(\mathbf{k}) \Psi_{\mathbf{k}} / 2, \quad (5)$$

where

$$\mathcal{H}(\mathbf{k}) = \begin{pmatrix} \mathcal{E}(\mathbf{k}) & \Delta(\mathbf{k}) \\ \Delta^\dagger(\mathbf{k}) & -\mathcal{E}^\dagger(-\mathbf{k}) \end{pmatrix} \quad (6)$$

and $\Psi_{\mathbf{k}} = (c_{\mathbf{k}sl}, c_{-\mathbf{k}sl}^\dagger)^t$. Here, $c_{\mathbf{k}sl}$ is the annihilation operator of electrons with momentum $\mathbf{k} = (k_x, k_y)$, spin angular momentum degree of freedom $s \in \{\uparrow, \downarrow\}$, and orbital angular momentum degree of freedom $\ell \in \{1, \dots, N\}$. $\mathcal{E}(\mathbf{k})$ is the Hamiltonian of the normal state, and $\Delta(\mathbf{k})$ is the gap function of the superconductor.

We consider a normal state with a mirror symmetry, corresponding to $\mathcal{E}(\mathbf{k})$ satisfying the relation $\mathcal{M}_{xy} \mathcal{E}(\mathbf{k}) \mathcal{M}_{xy}^\dagger = \mathcal{E}(\mathbf{k})$, where \mathcal{M}_{xy} is the matrix representation of the mirror operation taking $z \rightarrow -z$.

The superconducting state possesses a corresponding mirror symmetry as well if the gap function $\Delta(\mathbf{k})$ satisfies $\mathcal{M}_{xy} \Delta(\mathbf{k}) \mathcal{M}_{xy}^\dagger = \pm \Delta(\mathbf{k})$. The matrix Hamiltonian $\mathcal{H}(\mathbf{k})$ of the superconducting state then satisfies

$$\tilde{\mathcal{M}}_{xy}^\pm \mathcal{H}(\mathbf{k}) (\tilde{\mathcal{M}}_{xy}^\pm)^\dagger = \mathcal{H}(\mathbf{k}), \quad (7)$$

where

$$\tilde{\mathcal{M}}_{xy}^\pm = \begin{pmatrix} \mathcal{M}_{xy} & 0 \\ 0 & \pm \mathcal{M}_{xy}^* \end{pmatrix}, \quad (8)$$

and $\tilde{\mathcal{M}}_{xy}^\pm$ is the generalized mirror operator of the superconductor corresponding to the normal state mirror operator \mathcal{M}_{xy} . Since $\mathcal{H}(\mathbf{k})$ commutes with $\tilde{\mathcal{M}}_{xy}^\pm$, $\mathcal{H}(\mathbf{k})$ is block-diagonal in the basis in which $\tilde{\mathcal{M}}_{xy}^\pm$ is diagonal, with each block possessing a definite eigenvalue of $\tilde{\mathcal{M}}_{xy}^\pm$.

We now show that, with an additional constraint on the gap function, individual mirror subsectors of the superconducting state inherit \mathcal{C}' symmetry when the full Hamiltonian possesses \mathcal{C}' symmetry. Let the full Hamiltonian $\mathcal{H}(\mathbf{k})$ also possess a mirror symmetry denoted by $\tilde{\mathcal{M}}_{xy}^\pm$. For now, we will suppress the \pm and write $\tilde{\mathcal{M}}_{xy}$. A mirror subsector of $\tilde{\mathcal{M}}_{xy}$ possesses \mathcal{C}' symmetry if and only if a state $|u(\mathbf{k})\rangle$ and its \mathcal{C}' conjugate $|u^*(\mathbf{k})\rangle$ each have $\tilde{\mathcal{M}}_{xy}$ eigenvalue λ .

Therefore, we have

$$\tilde{\mathcal{M}}_{xy} |u(\mathbf{k})\rangle = \lambda |u(\mathbf{k})\rangle \quad (9)$$

and may write

$$\begin{aligned}\tilde{\mathcal{M}}_{xy}|u(\mathbf{k})\rangle &= \tilde{\mathcal{M}}_{xy}\mathcal{C}'|u^*(\mathbf{k})\rangle \\ &= \lambda\mathcal{C}'|u^*(\mathbf{k})\rangle \\ &= \mathcal{C}'\lambda|u^*(\mathbf{k})\rangle.\end{aligned}\quad (10)$$

Enforcing \mathcal{C}' symmetry in the mirror $\tilde{\mathcal{M}}_{xy}$ subsector, we also have

$$\tilde{\mathcal{M}}_{xy}|u^*(\mathbf{k})\rangle = \lambda|u^*(\mathbf{k})\rangle \quad (11)$$

Then Eq. 10 can be written as

$$\tilde{\mathcal{M}}_{xy}|u(\mathbf{k})\rangle = \mathcal{C}'\tilde{\mathcal{M}}_{xy}|u^*(\mathbf{k})\rangle \quad (12)$$

Using these expressions, we can write

$$\mathcal{C}'\tilde{\mathcal{M}}_{xy}|u^*(\mathbf{k})\rangle = \tilde{\mathcal{M}}_{xy}|u(\mathbf{k})\rangle \quad (13)$$

$$\mathcal{C}'\tilde{\mathcal{M}}_{xy}|u^*(\mathbf{k})\rangle = (\tilde{\mathcal{M}}_{xy}^*\tilde{\mathcal{M}})\tilde{\mathcal{M}}_{xy}|u(\mathbf{k})\rangle \quad (14)$$

$$\mathcal{C}'\tilde{\mathcal{M}}_{xy}|u^*(\mathbf{k})\rangle = \lambda^2\tilde{\mathcal{M}}_{xy}^*|u(\mathbf{k})\rangle \quad (15)$$

$$\mathcal{C}'\tilde{\mathcal{M}}_{xy}|u^*(\mathbf{k})\rangle = \lambda^2\tilde{\mathcal{M}}_{xy}^*\mathcal{C}'|u^*(\mathbf{k})\rangle \quad (16)$$

$$\mathcal{C}'\tilde{\mathcal{M}}_{xy} = \lambda^2\tilde{\mathcal{M}}_{xy}^*\mathcal{C}' \quad (17)$$

$$\mathcal{C}'\tilde{\mathcal{M}}_{xy}(\mathcal{C}')^\dagger = \lambda^2\tilde{\mathcal{M}}_{xy}^* \quad (18)$$

arriving at a constraint for a mirror subsector to inherit \mathcal{C}' symmetry that is the same as the constraint for a mirror subsector to inherit particle-hole symmetry \mathcal{C} [47]. This constraint is only satisfied for $\tilde{\mathcal{M}}_{xy}^-$. Thus, in superconductors with \mathcal{C}' symmetry and $\tilde{\mathcal{M}}_{xy}^-$, the \mathcal{C}' symmetry of the full Hamiltonian is inherited by each $\tilde{\mathcal{M}}_{xy}^-$ subsector. For the rest of this work, we therefore assume $\mathcal{H}(\mathbf{k})$ is invariant under $\tilde{\mathcal{M}}_{xy}^-$ and suppress the minus sign, working with $\tilde{\mathcal{M}}_{xy}$.

We now define the mirror Skyrmion number, the Skyrmion number computed over the two-dimensional Brillouin zone as defined previously, but using only occupied states within a single mirror subsector. A topological phase can then be constructed as a system with non-trivial Skyrmion number \mathcal{Q} in one mirror subsector, and non-trivial Skyrmion number $-\mathcal{Q}$ in the other subsector, in analogy to the construction of the quantum spin Hall insulator as a system with a Chern insulator with total Chern number $\mathcal{C} \neq 0$ in one spin subsector, and a second Chern insulator with total Chern number $-\mathcal{C}$ in the other spin subsector.

We can generalize these results to three-dimensional systems: the matrix Hamiltonian of the superconducting state then satisfies

$$\tilde{\mathcal{M}}_{xy}\mathcal{H}(k_x, k_y, k_z)\tilde{\mathcal{M}}_{xy}^\dagger = \mathcal{H}(k_x, k_y, -k_z), \quad (19)$$

and mirror Skyrmion numbers can be computed in the $k_x - k_y$ planes where $k_z = 0$ or π , as is done for mirror Chern numbers [47].

Sr₂RuO₄ as a candidate for realization of homotopic topological insulator phases.—We consider a model for Sr₂RuO₄ on the square lattice [48] also previously used to study topological crystalline superconductivity in this system [47]. This

model includes conduction electrons of the 4d t_{2g} orbitals of Ru, d_{yz} , d_{xz} , and d_{xy} .

The superconducting state of Sr₂RuO₄ is then described by the normal state Hamiltonian $\mathcal{H} = \mathcal{H}_{\text{kin}} + \mathcal{H}_{\text{soc}} + \mathcal{H}_B$ and gap function $\mathcal{H}_{\text{pair}}$ where

$$\mathcal{H}_{\text{kin}} = \sum_{\mathbf{k}s} \Psi_{\mathbf{k},s}^\dagger \mathcal{H}_{\text{kin}} \Psi_{\mathbf{k},s} \quad (20)$$

$$\mathcal{H}_{\text{soc}} = i\lambda \sum_{\ell mn} \varepsilon_{\ell mn} \sum_{\mathbf{k}ss'} c_{\mathbf{k}sl}^\dagger c_{\mathbf{k}sm} c_{\mathbf{k}ss'} \sigma_{ss'}^n \quad (21)$$

$$\mathcal{H}_B = -\mu_B H_z \sum_{k\ell ss'} c_{\mathbf{k}sl}^\dagger c_{\mathbf{k}ss'} \sigma_{ss'}^z \quad (22)$$

$$\mathcal{H}_{\text{pair}} = \frac{1}{2} \sum_{k\ell ss'} \hat{\Delta}_{ss'}^\ell(\mathbf{k}) c_{\mathbf{k}sl}^\dagger c_{-\mathbf{k}ss'}^\dagger, \quad (23)$$

with $\Psi_{\mathbf{k},s}^\dagger = (c_{\mathbf{k},s,yz}^\dagger, c_{\mathbf{k},s,xz}^\dagger, c_{\mathbf{k},s,xy}^\dagger)$ and

$$\mathcal{H}_{\text{kin}} = \begin{pmatrix} \epsilon_{\mathbf{k},yz} & g_{\mathbf{k}} & 0 \\ g_{\mathbf{k}} & \epsilon_{\mathbf{k},xz} & 0 \\ 0 & 0 & \epsilon_{\mathbf{k},xy} \end{pmatrix}. \quad (24)$$

Here, taking lattice spacing constant $a = 1$ throughout,

$$\epsilon_{\mathbf{k},yz} = -2t_1 \cos(k_y) - \mu \quad (25)$$

$$\epsilon_{\mathbf{k},xz} = -2t_1 \cos(k_x) - \mu \quad (26)$$

$$\begin{aligned}\epsilon_{\mathbf{k},xy} = -2t_2 (\cos(k_x) + \cos(k_y)) \\ - 4t_3 \cos(k_x) \cos(k_y) - \mu'\end{aligned} \quad (27)$$

and $g_{\mathbf{k}} = -4t_4 \sin(k_x) \sin(k_y)$. $\hat{\Delta}^\ell(\mathbf{k}) = i\Delta^\ell \mathbf{d}(\mathbf{k}) \cdot \boldsymbol{\sigma} \sigma_y$, with the d -vector $\mathbf{d}(\mathbf{k})$ assumed to be $\mathbf{d}(\mathbf{k}) = \hat{x} \sin(k_y) - \hat{y} \sin(k_x)$ as in Ueno *et al.* [47]. Other d -vectors are possible for the high-field phase and these will be considered in future work.

This model Hamiltonian for Sr₂RuO₄ considered by Ueno *et al.* [47] in the presence of an applied Zeeman field of strength H_z along the \hat{z} -axis of Sr₂RuO₄ (equivalent to the \hat{z} -axis in this work) is known to have particle-hole symmetry \mathcal{C} . However, we report here that it also possesses the generalized particle-hole symmetry \mathcal{C}' required for non-trivial homotopy group $\pi_2(\text{Sp}(2N)/\text{U}(N))$. As well, the normal state has mirror symmetry $\mathcal{M}_{xy} = \text{diag}(-i\sigma_z, -i\sigma_z, i\sigma_z)$ in the basis chosen for this work. In the high-field phase, furthermore, when the gap function is odd under the mirror operation \mathcal{M}_{xy} taking z to $-z$, \mathcal{C}' is inherited by each $\tilde{\mathcal{M}}_{xy}$ subsector. The low-field phase gap function is even under \mathcal{M}_{xy} , and, correspondingly, the $\tilde{\mathcal{M}}_{xy}$ subsectors do not inherit \mathcal{C}' symmetry.

We compute the mirror Skyrmion number for each $\tilde{\mathcal{M}}_{xy}$ subsector as a function of spin-orbit coupling λ and Zeeman coupling expressed as $\mu_B H_z$, while keeping other model parameters fixed to those used to model Sr₂RuO₄ specifically in past work [47]: $t_1 = t_2 = 0.5$, $t_3 = 0.2$, $t_4 = 0.1$, $\mu = -0.2$, $\mu' = -0.2$, and $\Delta^\ell = 0.6$ for each value of ℓ (yz , xz , and xy).

Characterization of homotopic topology in Sr₂RuO₄.—To compute mirror Skyrmion numbers for the $\tilde{\mathcal{M}}_{xy}$ subsectors of the Sr₂RuO₄ Hamiltonian, we proceed as follows: in the basis in which $\tilde{\mathcal{M}}_{xy}$ is diagonal,

the model for Sr_2RuO_4 is block-diagonal in the high-field phase. These blocks may be written as $\tilde{\mathcal{H}}_1(\mathbf{k})$ and $\tilde{\mathcal{H}}_2(\mathbf{k})$, with corresponding basis vectors $\Psi_1(\mathbf{k}) = \{c_{-\mathbf{k},xy,\uparrow}^\dagger, c_{-\mathbf{k},xz,\downarrow}^\dagger, c_{-\mathbf{k},yz,\downarrow}^\dagger, c_{\mathbf{k},xy,\uparrow}, c_{\mathbf{k},xz,\downarrow}, c_{\mathbf{k},yz,\downarrow}\}^t$, and $\Psi_2(\mathbf{k}) = \{c_{-\mathbf{k},xy,\downarrow}^\dagger, c_{-\mathbf{k},xz,\uparrow}^\dagger, c_{-\mathbf{k},yz,\uparrow}^\dagger, c_{\mathbf{k},xy,\downarrow}, c_{\mathbf{k},xz,\uparrow}, c_{\mathbf{k},yz,\uparrow}\}^t$, respectively, bases which naturally result from changing to the basis in which $\tilde{\mathcal{M}}_{xy}$ is diagonal. $\tilde{\mathcal{H}}_1(\mathbf{k})$ and $\tilde{\mathcal{H}}_2(\mathbf{k})$ each inherit \mathcal{C}' symmetry as well as \mathcal{C} symmetry.

We can construct angular momentum operators for these $\tilde{\mathcal{M}}_{xy}$ subsectors. First, the orbital angular momentum operator for our bases is $\tilde{\mathcal{L}} = \langle \tilde{\mathcal{L}}_x, \tilde{\mathcal{L}}_y, \tilde{\mathcal{L}}_z \rangle$, with

$$\tilde{\mathcal{L}}_i = \begin{pmatrix} -\mathcal{L}_i^* & 0 \\ 0 & \mathcal{L}_i \end{pmatrix}. \quad (28)$$

and $i \in \{x, y, z\}$. The corresponding normal state orbital angular momentum operator written in the basis of the t_{2g} orbitals xy , xz and yz [49] is $\mathcal{L} = \langle \mathcal{L}_x, \mathcal{L}_y, \mathcal{L}_z \rangle$, where

$$\mathcal{L}_x = \begin{pmatrix} 0 & -i & 0 \\ i & 0 & 0 \\ 0 & 0 & 0 \end{pmatrix}, \quad \mathcal{L}_y = \begin{pmatrix} 0 & 0 & i \\ 0 & 0 & 0 \\ -i & 0 & 0 \end{pmatrix},$$

$$\mathcal{L}_z = \begin{pmatrix} 0 & 0 & 0 \\ 0 & 0 & -i \\ 0 & i & 0 \end{pmatrix}. \quad (29)$$

Each $\tilde{\mathcal{M}}_{xy}$ subsector also retains a spin degree of freedom, however, due to the xy being even under \mathcal{M}_{xy} and the yz and xz orbitals being odd under \mathcal{M}_{xy} . Despite non-negligible spin-orbit coupling, orbital angular momentum and spin angular momentum are individually conserved in the $\tilde{\mathcal{M}}_{xy}$ subsectors. While the orbital angular momentum operators of the normal state are generators of the Lie group $\text{SO}(3)$, the spin angular momentum operators in the \hat{x} -, \hat{y} - and \hat{z} -directions of the normal state are generalizations of the corresponding spin operators of $\text{SU}(2)$, constructed from linear combinations of generators of the Lie group $\text{SU}(3)$ [50]. The basis of $\tilde{\mathcal{H}}_{1(2)}(\mathbf{k})$ corresponds to spin operators $\tilde{\mathcal{S}}_{1(2)} = \langle \tilde{\mathcal{S}}_{1(2),x}, \tilde{\mathcal{S}}_{1(2),y}, \tilde{\mathcal{S}}_{1(2),z} \rangle$, where

$$\tilde{\mathcal{S}}_{1(2),i} = \begin{pmatrix} -\mathcal{S}_{1(2),i}^* & 0 \\ 0 & \mathcal{S}_{1(2),i} \end{pmatrix}. \quad (30)$$

Here, the corresponding normal state spin operator is $\mathcal{S}_{1(2)} = \langle \mathcal{S}_{1(2),x}, \mathcal{S}_{1(2),y}, \mathcal{S}_{1(2),z} \rangle$, where

$$\mathcal{S}_{1,x} = \frac{1}{2} \begin{pmatrix} 0 & 1 & 1 \\ 1 & 0 & 1 \\ 1 & 1 & 0 \end{pmatrix}, \quad \mathcal{S}_{1,y} = \frac{1}{2} \begin{pmatrix} 0 & -i & -i \\ i & 0 & -i \\ i & i & 0 \end{pmatrix},$$

$$\mathcal{S}_{1,z} = \frac{1}{2} \begin{pmatrix} 2 & 0 & 0 \\ 0 & -1 & 0 \\ 0 & 0 & -1 \end{pmatrix}. \quad (31)$$

$\tilde{\mathcal{S}}_2$ can then be expressed in terms of $\tilde{\mathcal{S}}_1$ using the relations $\mathcal{S}_{2,x} = \mathcal{S}_{1,x}$, $\mathcal{S}_{2,y} = -\mathcal{S}_{1,y}$, and $\mathcal{S}_{2,z} = -\mathcal{S}_{1,z}$, since the raising operator for $\tilde{\mathcal{H}}_1(\mathbf{k})$ is the lowering operator for $\tilde{\mathcal{H}}_2(\mathbf{k})$ and vice versa.

Numerical results.—The total mirror Chern number for $\tilde{\mathcal{H}}_1(\mathbf{k})$ and the total mirror Chern number for $\tilde{\mathcal{H}}_2(\mathbf{k})$ as defined in Ueno *et al.* [47] are shown in Fig. 1 (a) and (b), respectively, computed as functions of spin-orbit coupling constant λ and applied Zeeman field $\mu_B H_z$. These are to be compared with the mirror Skyrmion number of $\tilde{\mathcal{H}}_1(\mathbf{k})$ and the mirror Skyrmion number of $\tilde{\mathcal{H}}_2(\mathbf{k})$, computed using $\tilde{\mathcal{S}}_1$ and $\tilde{\mathcal{S}}_2$, respectively, as functions of spin-orbit coupling constant λ and applied Zeeman field $\mu_B H_z$ shown in Fig. 1 (c) and (d). Mirror Skyrmion numbers computed using these spin operators show quantization to integer values throughout large regions of the phase diagrams, as well as some regions with smooth phase transitions, which will be discussed in greater detail in the next section. Skyrmion numbers computed using the orbital angular momentum operator are unquantized and trivial, in contrast. Noise in the Skyrmion number phase diagrams is due to extreme features in the Skyrmion number integrand $\Omega_\mathbf{k}$ that can occur over very small regions of momentum-space, necessitating a very fine \mathbf{k} -mesh using known methods.

For a given mirror subsector, \mathcal{Q} differs in value from \mathcal{C} and \mathcal{Q} can be non-zero when \mathcal{C} is zero and vice versa. \mathcal{Q} for $\tilde{\mathcal{H}}_{1(2)}(\mathbf{k})$ can be non-zero when \mathcal{Q} for $\tilde{\mathcal{H}}_{2(1)}(\mathbf{k})$ is zero, corresponding to the chiral topological Skyrmion insulator phase. This chiral topological Skyrmion insulator phase of matter occurs for model parameters previously used to model Sr_2RuO_4 specifically ($\lambda = 0.3$ and $\mu_B H_z = 0.1$), indicating Sr_2RuO_4 is a candidate for the chiral homotopic topological insulator phase of matter. In the case of Sr_2RuO_4 , the mirror Chern numbers are also non-zero, indicative of two distinct topologically non-trivial phases co-existing. The potential for interaction between these two distinct forms of non-trivial topology is an interesting direction for future work.

In the region of the phase diagram highlighted by a dashed line in Fig. 1 (c), \mathcal{Q} for $\tilde{\mathcal{H}}_1(\mathbf{k})$ is quantized to +2 while \mathcal{Q} for $\tilde{\mathcal{H}}_2(\mathbf{k})$ is quantized to -2. While time-reversal symmetry is broken in this region of the phase diagram, this phase is analogous to the quantum spin Hall phase constructed as two Chern insulators, one with Chern number $\mathcal{C} > 0$ and the other with Chern number $-\mathcal{C}$, so we call it the helical topological Skyrmion insulator phase of matter. We note that this phase suggests a time-reversal symmetric realization of the helical topological Skyrmion insulator phase is likely possible, that is topologically-equivalent to the helical topological Skyrmion insulator phase shown here.

Nature of the phase transitions.—We observe at least three kinds of phase transitions, two of which correspond to effectively discrete changes in the Skyrmion number according to the numerics. To better understand these two kinds, we study the momentum space ground state spin textures at points α , β and κ in Fig. 1 (c), shown in Fig. 2. We find individual skyrmions with $|\mathcal{Q}| > 1$ occur at α and β as shown in Fig. 2 (a) and (d) for α and (b) and (e) for β , respectively. The momentum space ground state spin texture at point κ , shown in Fig. 2 (c) and (f) instead consists of two features that gradually merge as \mathcal{Q} transitions from 2 to 0 for $\lambda = 0.6$ and increasing $\mu_B H_z$. This indicates that topological phase transitions occur only for certain kinds of Skyrmionic spin textures in the momentum-space Brillouin zone.

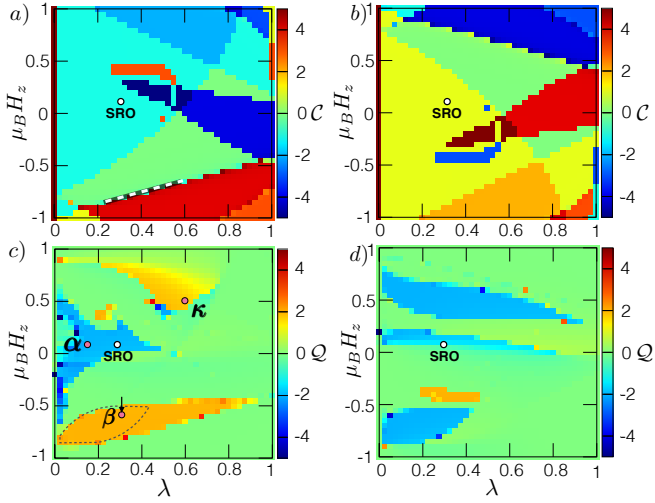


FIG. 1. Mirror Chern number \mathcal{C} computed as a function of spin-orbit coupling λ and applied Zeeman field $\mu_B H_z$ with step $\Delta k_i = \frac{\pi}{150}$ in momentum-space ($i \in \{x, y\}$) for $\tilde{\mathcal{H}}_1(\mathbf{k})$ in subfigure (a) and for $\tilde{\mathcal{H}}_2(\mathbf{k})$ in subpanel (b), respectively. Mirror Skyrmion number \mathcal{Q} computed as a function of spin-orbit coupling λ and applied Zeeman field $\mu_B H_z$ with step $\Delta k_i = \frac{\pi}{500}$ in momentum-space ($i \in \{x, y\}$) for $\tilde{\mathcal{H}}_1(\mathbf{k})$ in subpanel (c) and for $\tilde{\mathcal{H}}_2(\mathbf{k})$ in subpanel (d), respectively. The parameter set corresponding to Sr_2RuO_4 is highlighted by the white dot. The three red dots in subfigure (c) show the positions in coordinate space used to compute the momentum space ground state spin textures in Fig. 2, with Fig. 2 (a) and (d) corresponding to point α , Fig. 2 (b) and (e) corresponding to point β , and Fig. 2 (c) and (f) corresponding to point κ , respectively. The dashed outline in (c) highlights the region of the phase diagram in which the helical topological Skyrmion insulator phase of matter is realized. The black arrow above point β shows the location of the cut shown in Fig. 3. The black and white dashed line in (a) highlights part of a longer boundary at which the superconducting gap closes. Other model parameters are fixed to those used to model Sr_2RuO_4 specifically in past work [47]: $t_1 = t_2 = 0.5$, $t_3 = 0.2$, $t_4 = 0.1$, $\mu = -0.2$, $\mu' = -0.2$, and $\Delta^\ell = 0.6$ for each value of ℓ (yz , xz , and xy).

The first two kinds of phase transitions are also distinct from one another. In one kind, the Skyrmion number can change with the closing of the superconducting gap, such as along the boundary partially highlighted by the black and white dashed line in Fig. 1 (a), which is expected to destabilize calculation of the spin operator, similar to destabilization of the Chern number calculation for individual electronic bands when the direct gap between them goes to zero at some point in the Brillouin zone. In the second kind, shown in Fig. 3 (a), neither the direct gaps between occupied bands nor the superconducting gap close, as shown in Fig. 3 (b). While a topological phase transition without the closing of the two-dimensional bulk gap is observed for the electric quadrupole insulator [18], it occurs with a closing of the one-dimensional bulk gap. Here, slab calculations show the one-dimensional bulk is gapless throughout the region containing sub-regions with non-trivial Skyrmion numbers, either for topologically non-trivial (non-zero Mirror Chern numbers) or trivial rea-

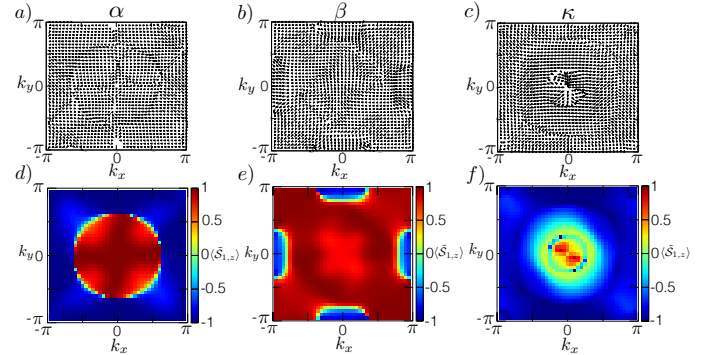


FIG. 2. Expectation values of the spin operators in the \hat{x} - and \hat{y} -directions for $\tilde{\mathcal{H}}_1(\mathbf{k})$, $\langle \hat{S}_{1,x} \rangle$ and $\langle \hat{S}_{1,y} \rangle$, respectively, plotted as a function of \mathbf{k} and renormalized to avoid overlap of the vectors as shown in (a), (b), and (c) and the expectation value of the spin operator in the \hat{z} -direction for $\tilde{\mathcal{H}}_1(\mathbf{k})$, $\langle \hat{S}_{1,z} \rangle$ is plotted as a function of \mathbf{k} and shown in (d), (e), and (f), with (a) and (d) computed for $\lambda = 0.15$ and $\mu_B H_z = 0.1$ and corresponding to point α in Fig. 1 (c), (b) and (e) computed for $\lambda = 0.3$ and $\mu_B H_z = -0.6$ and corresponding to point β in Fig. 1 (c), and (c) and (f) computed for $\lambda = 0.6$ and $\mu_B H_z = 0.5$ and corresponding to point κ in Fig. 1 (c).

sions. Thus, this type of phase transition occurs without closing of any energy gap.

While a gap closing is normally expected with a change in Skyrmion number in two-band models ($N = 1$), this situation is different from $N > 1$: there are multiple expressions for the Skyrmion number when it is locked to the Chern number, which better reveal why a gap closing is needed to destabilize the calculation in this special case. The integrand of this Skyrmion number for $N > 1$ does not take such forms, to our knowledge. Instead, the mirror Skyrmion number is destabilized by other changes in the case highlighted by the black arrow in Fig. 1 (c): the integrand of the mirror Skyrmion number $\Omega_{\mathbf{k}}$ during this phase transition changes at two points in the Brillouin zone related by symmetry, highlighted by white arrows in Fig. 4 (a) and (b) for two values of the applied Zeeman field $\mu_B H_z$ between which the change is very noticeable. The normalized spin texture in the vicinity of this point in the Brillouin zone is shown for the parameter set corresponding to Fig. 4 (a), revealing singularities in the derivative of the normalized ground state spin expectation value develop during the phase transition that destabilize the mirror Skyrmion number and permit a discrete change in its value.

Bulk-boundary correspondence and the entanglement spectrum.—Since some topological phase transitions can occur in this system without the closing of direct gaps, bulk-boundary correspondence does not necessarily hold for these topologically non-trivial phases. Thus, we do not expect gapless boundary states even for boundaries respecting \mathcal{C}' symmetry. Furthermore, the entanglement spectrum as it is currently computed is not appropriate for characterization of these topological phases: computation of the entanglement spectrum for a Hamiltonian relies on being able to adiabatically deform that Hamiltonian to a flat-band limit that we know is topologically equivalent to the original Hamiltonian [51–53]. The flat-band

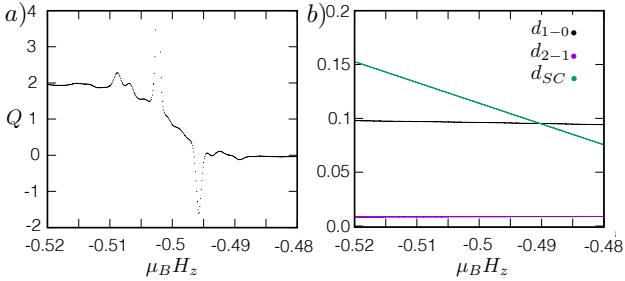


FIG. 3. (a) Mirror Skyrmiion number Q for $\tilde{\mathcal{H}}_1(\mathbf{k})$ computed as a function of applied Zeeman field $\mu_B H_z$ for fixed spin-orbit coupling value $\lambda = 0.3$ along the cut shown in Fig. 1 (c) with step $\Delta k_i = \frac{\pi}{300}$, with $i \in \{x, y\}$. (b) The minimum direct gap between the two lowest bands, d_{1-0} , the minimum direct gap between the second two lowest bands, d_{2-1} , and the minimum direct gap between the two middle bands and minimum direct superconducting gap, d_{SC} of $\tilde{\mathcal{H}}_1(\mathbf{k})$, each computed as a function of applied Zeeman field $\mu_B H_z$ for fixed spin-orbit coupling value $\lambda = 0.3$ along the cut shown in Fig. 1 (c) with step $\Delta k_i = \frac{\pi}{300}$, with $i \in \{x, y\}$.

limit counterpart of the Hamiltonian is only guaranteed to be topologically-equivalent to the original if topological phase transitions only occur with gap-closings. This further suggests that characterization of topological phases with the entanglement spectrum must be done with care: if the system is topologically non-trivial in whole or in part due to topology that can emerge via topological phase transitions without gap closings, the entanglement spectrum may no longer correspond to the topology of the original system.

Applications to Sr₂RuO₄ and other superconductors.—Recent Knight-shift experiments have further called into question the nature of the superconducting pairing in Sr₂RuO₄ [54, 55], but spin-triplet pairing in Sr₂RuO₄ remains a very strong possibility [56]. While the parameter set used here for Sr₂RuO₄ in the high-field phase is established by previous works, the topology realized for other \mathbf{d} vectors and further characterization of the parameter values relevant to Sr₂RuO₄ should be explored.

The helical topological Skyrmiion insulator phase, while occurring for a value of the spin-orbit coupling constant λ relevant to Sr₂RuO₄, occurs for strong Zeeman fields at which the parameter Δ of the superconducting gap function is expected to be zero in experiments. This work instead primarily serves as the introduction of this phase and its realization in a physically-relevant model, although the phase does persist to smaller $|\Delta|$.

The prevalence of the \mathcal{C}' symmetry in other systems and especially other superconductors is currently not known and this work serves as motivation for exploration of this topology in other systems and multi-orbital superconductors in particular. Given that \mathcal{C}' is the product of particle-hole symmetry \mathcal{C} and spatial inversion \mathcal{I} , however, it is expected to be fairly commonplace. This work also serves as further motivation and guidance in the search for counterpart higher-dimensional homotopic topological phases and homotopic topology characterized by other homotopy groups.

Bulk-boundary correspondence does not hold for these

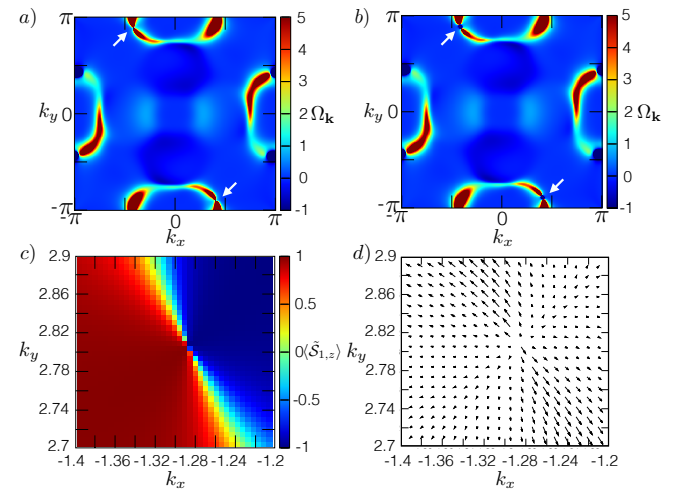


FIG. 4. Integrand of the mirror Skyrmiion number Q , Ω_k , as a function of momenta k_x and k_y in the Brillouin zone for spin-orbit coupling constant $\lambda = 0.3$ and applied Zeeman field coupling $\mu_B H_z = -0.5$ shown in (a) and $\mu_B H_z = -0.495$ shown in (b), respectively, two points in the phase diagram along the cut represented by a black arrow in Fig. 1 (c) and further analyzed in Fig. 3. Two small white arrows in each of (a) and (b) highlight the features (related by symmetry) in Ω_k that change during the topological phase transition. For $\mu_B H_z = -0.5$ and $\lambda = 0.3$ corresponding to (a), (c) shows the ground state expectation value of the component of the spin operator in the \hat{z} -direction, $\langle \hat{S}_{1,z} \rangle$ and (d) shows the corresponding expectation values of the components of the spin operator in the \hat{x} - and \hat{y} -directions, $\langle \hat{S}_{1,x} \rangle$ and $\langle \hat{S}_{1,y} \rangle$, renormalized to prevent overlap of the vectors.

topological phases, so experiments measuring tunneling conductance at a sample boundary are not expected to be relevant even for boundaries respecting \mathcal{C}' symmetry. However, past work shows defects can be used to realize mappings corresponding to non-trivial homotopy groups capable of trapping unpaired Majorana zero-modes [57]. Thus, these homotopic topological phases should be investigated for their potential to realize unpaired Majorana zero-modes, as well as for realizing such modes by different mechanisms. As well, inelastic neutron scattering may reveal signatures of the momentum-space Skyrmiions defining these topological phases.

In conclusion, we introduce a generalization of the Chern insulator for one-electron Hamiltonians with $2N \times 2N$ matrix representations and $N > 1$, the chiral topological Skyrmiion insulator, and a generalization of the quantum spin Hall insulator, the helical topological Skyrmiion insulator. These topological phases of matter are protected by a generalized particle-hole symmetry \mathcal{C}' corresponding to non-trivial homotopy group $\pi_2(Sp(2N)/U(N))$. They are characterized by a global topological invariant, the Skyrmiion number. For $N = 1$, the Skyrmiion number is equivalent to the Chern number, meaning these topological phases of matter distinct from the Chern insulator only exist for $N > 1$.

We find both phases are realized in an established tight-binding model describing spin-triplet superconductivity in Sr₂RuO₄. The chiral topological Skyrmiion insulator phase

is furthermore realized for a parameter set previously established for Sr_2RuO_4 in the high-field phase, indicating Sr_2RuO_4 may harbour homotopic topological physics in addition to topological crystalline superconductivity. Three different kinds of phase transitions are observed for the Skyrmiion number, two of which are discrete and topological, and one which is smooth, differentiated by the nature of the Skyrmiion in the momentum space ground state spin texture. Topological phase transitions can also occur with or without closing of direct gaps. When the Skyrmiion number changes without a closing of direct gaps involving occupied states, it is instead destabilized by singularities in the derivative of the normalized ground state spin expectation value at some points in momentum-space.

The construction of these homotopic topological phases of matter, reliant on a mirror symmetry and a generalized particle-hole symmetry, suggests the promise of *engineering* of topological phases of matter by considering multiple symmetries, and multiple methods of topological condensed matter physics, in combination. Rather than simply asking what is possible when a system possesses some set of symmetries, we can ask how different symmetries can be used together to realize novel topologically non-trivial phases of matter. As well, these results indicate additional care should be taken in characterizing topologically non-trivial phases of matter using the entanglement spectrum, and motivate the search for additional theoretical and experimental tools for probing non-trivial topology. More efficient methods for computing the

Skyrmiion number are especially desirable, as the topology can result from very delicate, extreme features in the Brillouin zone of the Skyrmiion number integrand $\Omega_{\mathbf{k}}$, as well as methods for computing the Skyrmiion number and other homotopy invariants in interacting systems. More generally, greater investigation of the consequences of this homotopic topological physics is also needed.

The possible realization of this non-trivial topology in Sr_2RuO_4 , an intensely-studied superconductor, further motivates review of past results on the material, as well as investigation of other superconductors as hosts to this physics given that the C' symmetry is likely commonplace. Inelastic neutron scattering experiments are promising for probing these phases, which exhibit topological magnetic order but for which the bulk-boundary correspondence does not apply. The potential for these topological phases to realize unpaired Majorana zero-modes by novel avenues, and potentially in what are seen as topologically trivial superconductors, is also an important direction for future work [57]. Analogous physics is also expected and should be sought in driven and dissipative systems as well as systems that are not electronic or not purely electronic.

We thank Y. B. Kim, J. Motruk, M. Sigrist, T. Schuster, M. Zaletel, D. Podolsky and S. Gazit for useful discussions. We especially wish to acknowledge J. E. Moore for many helpful discussions. A. M. C. also wishes to thank the Aspen Center for Physics, which is supported by National Science Foundation grant PHY-1066293, for hosting during some stages of this work. A. M. C. was supported by the NSERC PDF.

-
- [1] F. D. M. Haldane, "Model for a quantum Hall effect without landau levels: Condensed-matter realization of the "parity anomaly"," *Phys. Rev. Lett.* **61**, 2015–2018 (1988).
- [2] C. L. Kane and E. J. Mele, "Quantum spin hall effect in graphene," *Phys. Rev. Lett.* **95**, 226801 (2005).
- [3] C. L. Kane and E. J. Mele, " Z_2 topological order and the quantum spin hall effect," *Phys. Rev. Lett.* **95**, 146802 (2005).
- [4] B. Andrei Bernevig, Taylor L. Hughes, and Shou-Cheng Zhang, "Quantum spin Hall effect and topological phase transition in HgTe quantum wells," *Science* **314**, 1757–1761 (2006).
- [5] Markus König, Steffen Wiedmann, Christoph Brüne, Andreas Roth, Hartmut Buhmann, Laurens W. Molenkamp, Xiao-Liang Qi, and Shou-Cheng Zhang, "Quantum spin hall insulator state in hgte quantum wells," *Science* **318**, 766–770 (2007).
- [6] Joseph Maciejko, Taylor L. Hughes, and Shou-Cheng Zhang, "The quantum spin hall effect," *Annual Review of Condensed Matter Physics* **2**, 31–53 (2011).
- [7] A. A. Burkov and Leon Balents, "Weyl semimetal in a topological insulator multilayer," *Phys. Rev. Lett.* **107**, 127205 (2011).
- [8] S. A. Parameswaran, T. Grover, D. A. Abanin, D. A. Pesin, and A. Vishwanath, "Probing the chiral anomaly with nonlocal transport in three-dimensional topological semimetals," *Phys. Rev. X* **4**, 031035 (2014).
- [9] Su-Yang Xu, Ilya Belopolski, Nasser Alidoust, Madhab Neupane, Guang Bian, Chenglong Zhang, Raman Sankar, Guoqing Chang, Zhujun Yuan, Chi-Cheng Lee, Shin-Ming Huang, Hao Zheng, Jie Ma, Daniel S. Sanchez, BaoKai Wang, Arun Bansil, Fangcheng Chou, Pavel P. Shibayev, Hsin Lin, Shuang Jia, and M. Zahid Hasan, "Discovery of a weyl fermion semimetal and topological fermi arcs," *Science* **349**, 613–617 (2015).
- [10] Ling Lu, Zhiyu Wang, Dexin Ye, Lixin Ran, Liang Fu, John D. Joannopoulos, and Marin Soljacić, "Experimental observation of Weyl points," *Science* **349**, 622–624 (2015).
- [11] B. Q. Lv, H. M. Weng, B. B. Fu, X. P. Wang, H. Miao, J. Ma, P. Richard, X. C. Huang, L. X. Zhao, G. F. Chen, Z. Fang, X. Dai, T. Qian, and H. Ding, "Experimental discovery of Weyl semimetal TaAs," *Phys. Rev. X* **5**, 031013 (2015).
- [12] Binghai Yan and Claudia Felser, "Topological materials: Weyl semimetals," *Annual Review of Condensed Matter Physics* **8**, 337–354 (2017).
- [13] K. Kuroda, T. Tomita, M. T. Suzuki, C. Bareille, A. A. Nugroho, P. Goswami, M. Ochi, M. Ikhlas, M. Nakayama, S. Akebi, R. Noguchi, R. Ishii, N. Inami, K. Ono, H. Kumigashira, A. Varykhalov, T. Muro, T. Koretsune, R. Arita, S. Shin, Takeshi Kondo, and S. Nakatsuji, "Evidence for magnetic weyl fermions in a correlated metal," *Nature Materials* **16**, 1090 EP – (2017).
- [14] Liang Fu, "Topological crystalline insulators," *Phys. Rev. Lett.* **106**, 106802 (2011).
- [15] Timothy H. Hsieh, Hsin Lin, Junwei Liu, Wenhui Duan, Arun Bansil, and Liang Fu, "Topological crystalline insulators in the snte material class," *Nature Communications* **3**, 982 EP – (2012).
- [16] Yoichi Ando and Liang Fu, "Topological crystalline insulators and topological superconductors: From concepts to materials," *Annual Review of Condensed Matter Physics* **6**, 361–381

- (2015).
- [17] Barry Bradlyn, Jennifer Cano, Zhijun Wang, M. G. Vergniory, C. Felser, R. J. Cava, and B. Andrei Bernevig, “Beyond Dirac and Weyl fermions: Unconventional quasiparticles in conventional crystals,” *Science* **353** (2016).
- [18] Vladimir A. Benalcazar, B. Andrei Bernevig, and Taylor L. Hughes, “Quantized electric multipole insulators,” **357**, 61–66 (2017).
- [19] Benjamin J. Wieder, Barry Bradlyn, Zhijun Wang, Jennifer Cano, Youngkuk Kim, Hyeong-Seok D. Kim, Andrew M. Rappe, C. L. Kane, and B. Andrei Bernevig, “Wallpaper fermions and the nonsymmorphic dirac insulator,” **361**, 246–251 (2018).
- [20] Alexander B. Khanikaev, S. Hossein Mousavi, Wang-Kong Tse, Mehdi Kargarian, Allan H. MacDonald, and Gennady Shvets, “Photonic topological insulators,” *Nature Materials* **12**, 233 EP – (2012).
- [21] Roman Süsstrunk and Sebastian D. Huber, “Observation of phononic helical edge states in a mechanical topological insulator,” **349**, 47–50 (2015).
- [22] Lisa M. Nash, Dustin Kleckner, Alismari Read, Vincenzo Vitelli, Ari M. Turner, and William T. M. Irvine, “Topological mechanics of gyroscopic metamaterials,” **112**, 14495–14500 (2015).
- [23] Ching Hua Lee, Stefan Imhof, Christian Berger, Florian Bayer, Johannes Brehm, Laurens W. Molenkamp, Tobias Kiessling, and Ronny Thomale, “Topoelectrical circuits,” *Communications Physics* **1**, 39 (2018).
- [24] Wang Yao, A. H. MacDonald, and Qian Niu, “Optical control of topological quantum transport in semiconductors,” *Phys. Rev. Lett.* **99**, 047401 (2007).
- [25] Takashi Oka and Hideo Aoki, “Photovoltaic hall effect in graphene,” *Phys. Rev. B* **79**, 081406 (2009).
- [26] Takuya Kitagawa, Erez Berg, Mark Rudner, and Eugene Demler, “Topological characterization of periodically driven quantum systems,” *Phys. Rev. B* **82**, 235114 (2010).
- [27] Netanel H. Lindner, Gil Refael, and Victor Galitski, “Floquet topological insulator in semiconductor quantum wells,” *Nature Physics* **7**, 490–495 (2011).
- [28] Jrme Cayssol, Balzs Dra, Ferenc Simon, and Roderich Moessner, “Floquet topological insulators,” *physica status solidi (RRL) Rapid Research Letters* **7**, 101–108.
- [29] Mark S. Rudner, Netanel H. Lindner, Erez Berg, and Michael Levin, “Anomalous edge states and the bulk-edge correspondence for periodically driven two-dimensional systems,” *Phys. Rev. X* **3**, 031005 (2013).
- [30] A. Gómez-León and G. Platero, “Floquet-bloch theory and topology in periodically driven lattices,” *Phys. Rev. Lett.* **110**, 200403 (2013).
- [31] Rahul Roy and Fenner Harper, “Floquet topological phases with symmetry in all dimensions,” *Phys. Rev. B* **95**, 195128 (2017).
- [32] Takashi Oka and Sota Kitamura, “Floquet engineering of quantum materials,” *Annual Review of Condensed Matter Physics* **10**, 387–408 (2019).
- [33] Vedika Khemani, Achilleas Lazarides, Roderich Moessner, and S. L. Sondhi, “Phase structure of driven quantum systems,” *Phys. Rev. Lett.* **116**, 250401 (2016).
- [34] Huitao Shen, Bo Zhen, and Liang Fu, “Topological band theory for non-hermitian hamiltonians,” *Phys. Rev. Lett.* **120**, 146402 (2018).
- [35] Shunyu Yao and Zhong Wang, “Edge states and topological invariants of non-hermitian systems,” *Phys. Rev. Lett.* **121**, 086803 (2018).
- [36] Shunyu Yao, Fei Song, and Zhong Wang, “Non-hermitian chern bands,” *Phys. Rev. Lett.* **121**, 136802 (2018).
- [37] Flore K. Kunst, Elisabet Edvardsson, Jan Carl Budich, and Emil J. Bergholtz, “Biorthogonal bulk-boundary correspondence in non-hermitian systems,” *Phys. Rev. Lett.* **121**, 026808 (2018).
- [38] Huitao Shen and Liang Fu, “Quantum oscillation from in-gap states and a non-hermitian landau level problem,” *Phys. Rev. Lett.* **121**, 026403 (2018).
- [39] Zongping Gong, Yuto Ashida, Kohei Kawabata, Kazuaki Takasan, Sho Higashikawa, and Masahito Ueda, “Topological phases of non-hermitian systems,” *Phys. Rev. X* **8**, 031079 (2018).
- [40] Kohei Kawabata, Sho Higashikawa, Zongping Gong, Yuto Ashida, and Masahito Ueda, “Topological unification of time-reversal and particle-hole symmetries in non-hermitian physics,” *Nature Communications* **10**, 297 (2019).
- [41] J. E. Avron, R. Seiler, and B. Simon, “Homotopy and quantization in condensed matter physics,” *Phys. Rev. Lett.* **51**, 51–53 (1983).
- [42] Chunxiao Liu, Farzan Vafa, and Cenke Xu, “Symmetry-protected topological Hopf insulator and its generalizations,” *Phys. Rev. B* **95**, 161116 (2017).
- [43] Raoul Bott, “The stable homotopy of the classical groups,” *Annals of Mathematics* **70**, 313–337 (1959).
- [44] Mamoru Mimura and Hiroshi Toda, “Homotopy groups of symplectic groups,” *J. Math. Kyoto Univ.* **3**, 251–273 (1963).
- [45] Joel E. Moore, Ying Ran, and Xiao-Gang Wen, “Topological surface states in three-dimensional magnetic insulators,” *Phys. Rev. Lett.* **101**, 186805 (2008).
- [46] Florian Loder, Arno P. Kampf, Thilo Kopp, and Daniel Braak, “Momentum-space spin texture in a topological superconductor,” *Phys. Rev. B* **96**, 024508 (2017).
- [47] Yuji Ueno, Ai Yamakage, Yukio Tanaka, and Masatoshi Sato, “Symmetry-protected majorana fermions in topological crystalline superconductors: Theory and application to sr_2ruo_4 ,” *Phys. Rev. Lett.* **111**, 087002 (2013).
- [48] K. K Ng and M Sigrist, “The role of spin-orbit coupling for the superconducting state in sr_2ruo_4 ,” *Europhysics Letters (EPL)* **49**, 473–479 (2000).
- [49] Georgios L. Stamokostas and Gregory A. Fiete, “Mixing of $t_{2g} - e_g$ orbitals in 4d and 5d transition metal oxides,” *Phys. Rev. B* **97**, 085150 (2018).
- [50] H. Georgi, *Lie Algebras In Particle Physics: from Isospin To Unified Theories*, Frontiers in Physics (Avalon Publishing, 1999).
- [51] Hui Li and F. D. M. Haldane, “Entanglement spectrum as a generalization of entanglement entropy: Identification of topological order in non-abelian fractional quantum hall effect states,” *Phys. Rev. Lett.* **101**, 010504 (2008).
- [52] Ingo Peschel and Viktor Eisler, “Reduced density matrices and entanglement entropy in free lattice models,” *Journal of Physics A: Mathematical and Theoretical* **42**, 504003 (2009).
- [53] Lukasz Fidkowski and Alexei Kitaev, “Effects of interactions on the topological classification of free fermion systems,” *Phys. Rev. B* **81**, 134509 (2010).
- [54] A. Pustogow, Yongkang Luo, A. Chronister, Y.-S. Su, D. A. Sokolov, F. Jerzembeck, A. P. Mackenzie, C. W. Hicks, N. Kikugawa, S. Raghu, E. D. Bauer, and S. E. Brown, arXiv: 1904.00047.
- [55] Astrid Rmer, D D. Scherer, I M. Eremin, Peter Hirschfeld, and Brian Andersen, arXiv: 1905.04782.
- [56] Andrew P. Mackenzie, Thomas Scaffidi, Clifford W. Hicks, and Yoshiteru Maeno, “Even odder after twenty-three years: the superconducting order parameter puzzle of Sr_2RuO_4 ,” *npj Quantum Materials* **5**, 10001 (2020).

tum Materials **2**, 40 (2017).
[57] Zhongbo Yan, Ren Bi, and Zhong Wang, “Majorana zero

modes protected by a hopf invariant in topologically trivial superconductors,” Phys. Rev. Lett. **118**, 147003 (2017).